

See discussions, stats, and author profiles for this publication at: <https://www.researchgate.net/publication/10586490>

Conformational analysis of furanoid epsilon-sugar amino acid containing cyclic peptides by NMR spectroscopy, molecular dynamics simulation, and X-ray crystallography: Evidence for...

ARTICLE in JOURNAL OF THE AMERICAN CHEMICAL SOCIETY · OCTOBER 2003

Impact Factor: 12.11 · DOI: 10.1021/ja035461+ · Source: PubMed

CITATIONS

53

READS

66

12 AUTHORS, INCLUDING:



Mark Johan van Raaij

Spanish National Research Council

110 PUBLICATIONS **2,393** CITATIONS

SEE PROFILE



Antonio L. Llamas-Saiz

University of Santiago de Compostela

159 PUBLICATIONS **2,412** CITATIONS

SEE PROFILE



Antonio Lavecchia

University of Naples Federico II

119 PUBLICATIONS **2,473** CITATIONS

SEE PROFILE



Mark Overhand

Leiden University

110 PUBLICATIONS **2,769** CITATIONS

SEE PROFILE

Conformational Analysis of Furanoid ϵ -Sugar Amino Acid Containing Cyclic Peptides by NMR Spectroscopy, Molecular Dynamics Simulation, and X-ray Crystallography: Evidence for a Novel Turn Structure

Renate M. van Well,[†] Luciana Marinelli,[‡] Cornelis Altona,[†] Kees Erkelens,[†]
Gregg Siegal,[†] Mark van Raaij,^{†,§} Antonio L. Llamas-Saiz,[§] Horst Kessler,[‡]
Ettore Novellino,[‡] Antonio Lavecchia,[‡] Jacques H. van Boom,[†] and
Mark Overhand^{*,†}

Contribution from the Leiden Institute of Chemistry, Gorlaeus Laboratories, Leiden University, P.O. Box 9502, 2300 RA Leiden, The Netherlands, Institut für Organische Chemie und Biochemie, Technische Universität München, Lichtenbergstrasse 4, D-85747 Garching, Germany, Departamento de Bioquímica y Biología Molecular, Facultad de Farmacia, Unidad de Rayos X, Edificio CACTUS, Universidad de Santiago, 15782 Santiago de Compostela, Spain, and Dipartimento di Chimica Farmaceutica e Tossicologica, Università di Napoli "Federico II", Via D. Montesano 49, 80131 Napoli, Italy

Received April 4, 2003; E-mail: overhand@chem.leidenuniv.nl

Abstract: Sugar amino acids (SAAs) are useful building blocks for the design of peptidomimetics and peptide scaffolds. The three-dimensional structures of cyclic hybrid molecules containing the furanoid ϵ -SAA III and several amino acids were elucidated to study the preferred conformation of such an ϵ -SAA and its conformational influence on the backbone of cyclic peptides. NMR-based molecular dynamics simulations and empirical calculations of the cyclic tetramer **1**, consisting of two copies of the SAA residue and two amino acids, revealed that it is conformationally restrained. The two SAA residues adopt different conformations. One of them forms an unusual turn, stabilized by an intraresidue nine-member hydrogen bond. The methylene functionalities of the other SAA residue are positioned in such a way that an intraresidue H bond is not possible. The X-ray crystal structure of **1** strongly resembles the solution conformation. Molecular dynamics calculations in combination with NMR analysis were also performed for compounds **2** and **3**, which contain the RGD (Arg-Gly-Asp) consensus sequence and were previously shown to inhibit $\alpha_{IIb}\beta_3$ -receptor-mediated platelet aggregation. The biologically most active compound **2** adopts a preferred conformation with the single SAA residue folded into the nine-member H bond-containing turn. Compound **3**, containing an additional valine residue, as compared with compound **2**, is conformational flexible. Our studies demonstrate that the furanoid ϵ -SAA III is able to introduce an unusual intraresidue hydrogen bond-stabilized β -turn-like conformation in two of the three cyclic structures.

Introduction

Sugar amino acids (SAAs),¹ carbohydrate derivatives bearing an amino and a carboxylic acid functionality, are predominantly found in nature in the cell wall of bacteria (i.e., muraminic acid)² and as subunits of specific oligosaccharides (i.e., neuraminic acid).³ In addition, SAAs are found as components of antibiotics,

such as siastatin B⁴ and ezomycin A.⁵ As early as 1975, glycomimetics containing synthetic SAAs, having amide bonds rather than the glycosidic linkages, have been constructed.⁶ Several of these types of backbone-modified oligomers are able to adopt stable secondary structures.⁷ More recently, it was recognized that SAAs can not only serve as glycomimetics but also as conformational-restricted peptide isosteres.⁸ Because of the presence of a pyran or furan ring, SAAs have been found to induce turn structures when incorporated in linear or cyclic peptides. For instance, dipeptide isosteric pyranoid δ -SAAs **I** (Figure 1) have been shown by NMR techniques^{8h} and molecular dynamics (MD) calculations^{8a} to serve as a β -turn mimic.

[†] Leiden University.

[‡] Technische Universität München.

[§] Universidad de Santiago.

[‡] Università di Napoli "Federico II".

- (1) (a) Lohof, E.; Burkhart, F.; Born, M. A.; Planker, E.; Kessler, H. *Advances in Amino Acid Mimetics and Peptidomimetics*; Abell, A., Ed.; JAI Press, Inc.: Stamford, Connecticut, 1999; Vol. 2, p 263. (b) Gruner, S. A. W.; Locardi, E.; Lohof, E.; Kessler, H. *Chem. Rev.* **2002**, *102*, 491. (c) Schweizer, F. *Angew. Chem., Int. Ed.* **2002**, *41*, 230. (d) Chakraborty, T. K.; Ghosh, S.; Jayaprakash, S. *Curr. Med. Chem.* **2002**, *9*, 421. (e) Graf von Roeder, E.; Born, M. A.; Stöckle, M.; Kessler, H. *Synthesis of Peptides with Sugar Amino Acids*; Goodman, M., Ed.; In *Houben-Weyl*; Thieme: Stuttgart, 2003; Vol. E22c, p 807.
- (2) *Biochemistry*; Zubay, G., Ed.; Macmillan Publishing: New York, 1988; p 149.

(3) (a) Schauer, R. *Glycoconjugate J.* **2000**, *17*, 485. (b) Kiefel, M. J.; von Itzstein, M. *Chem. Rev.* **2002**, *102*, 471.

(4) Umezawa, H.; Aoyagi, T.; Komiyama, H.; Hamada, M.; Takeuchi, T. *J. Antibiot.* **1974**, *27*, 963.

(5) (a) Sakata, K.; Sakurai, A.; Tamura, S. *Tetrahedron Lett.* **1974**, *16*, 1533.

(b) Sakata, K.; Sakurai, A.; Tamura, S. *Tetrahedron Lett.* **1974**, *49*, 4327.

(6) Fuchs, E.; Lehman, J. *Carbohydr. Res.* **1976**, *49*, 267.

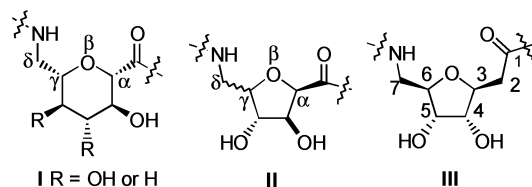


Figure 1. δ -SAAs of types I and II and ϵ -SAA III.

Detailed structural information has also been disclosed of furanoid δ -SAA II containing Leu-enkephalin analogues, in which the SAA residue is partly involved in a turn structure.^{8e} Several groups^{8f,9} have reported the synthesis of the one atom-homologated pyranoid and furanoid ϵ -SAAs; however, their preferred solution conformation and their influence on the three-dimensional structure of peptides have not been elucidated in detail.

Recently, we have constructed cyclic molecules **1**, **2**, and **3** (Figure 2) containing the furanoid ϵ -SAA 7-amino-3,6-anhydro-2,7-dideoxy-D-*allo*-heptonic acid (III, Figure 1) using a cyclization/cleavage strategy.¹⁰ Compound **1** contains two adjacent SAA residues and two aliphatic amino acids. Compounds **2** and **3** contain one SAA residue and correspond to a cyclic pentapeptide and hexapeptide, respectively, having an additional endocyclic carbon atom. The latter were shown to bind to integrin receptors¹¹ via the RGD (Arg-Gly-Asp) consensus sequence present in both molecules.^{10b}

We present here the conformational analysis of compounds **1–3** using NMR spectroscopy, distance geometry (DG), and subsequent MD calculations to explore the effect of SAA III on the conformation of cyclic peptides. In addition, the conformation of **1** in solution was compared with an X-ray structure and empirical calculations of the ring conformations in the SAA residues. To our knowledge, this is the first time that X-ray data is available for this kind of hybrid molecule, allowing a comparison with data obtained from PSEUROT as well as NMR-based MD calculations. From these data, it was concluded that the furanoid ϵ -SAA III is able to form a novel unusual turn conformation in small cyclic peptidic constructs.

Results

Conformational Analysis of cyclo[Phe-SAA-SAA-Ala] (**1**).

NMR Analysis. Analysis of the 1D spectrum of **1** reveals a single set of resonances, both at low (275 K) and high temperature (320 K). ¹H NMR as well as COSY, TOCSY, and ROESY spectra ($\tau_{\text{mix}} = 180$ ms) were used to unambiguously assign the complete resonance set. Diastereotopic assignment of the methylene protons present in the SAAs was accomplished on the basis of ROEs and coupling constants. A total of 35 well-resolved cross-peaks were found in the ROESY spectrum, most of which are either intraresidue or sequential. The presence of strong $\text{H}\alpha^i/\text{HN}^{i+1}$ ROEs and the absence of $\text{H}\alpha^i/\text{H}\alpha^{i+1}$ cross-peaks confirmed that all the amide bonds are in the trans conformation.¹² Two HN/HN cross-peaks were observed, one resulting from an interaction between the amide protons of SAA² and Phe¹, the other from an interaction between Phe¹ and Ala⁴. The amide proton of Ala⁴ has a very small coupling constant ($^3J_{\text{HN,H}\alpha} = 2.4$ Hz), as well as a large downfield shift (8.85 ppm) as compared to an alanine residue in a random coil (i.e., $\delta = 8.25$ ppm).¹³ The large downfield shift may be a conformational effect or due to a hydrogen-bonding interaction. The temperature dependence of the amide proton chemical shift of SAA² shows a small temperature gradient (-3.5 ppb/K, Table 1) compared to that of Phe¹HN and Ala⁴HN (-9.5 ppb/K and

Table 1. Temperature Coefficients of the Amide Protons of **1–3** in ppB/K

	Phe	SAA	SAA	Ala	
1	−9.5	−3.5	−5.6	−10.9	
	Arg	Gly	Asp	Val	SAA
2	−7.1	−8.8	−5.1	—	−1.6
3	−5.4	−6.8	−5.7	−4.3	−5.4

-10.9 ppb/K, respectively). The amide proton of SAA³ exhibits an intermediate temperature coefficient (-5.6 ppb/K). These values indicate that only the amide protons of the SAA residues are involved in intramolecular hydrogen bonding.¹⁴

- (7) (a) Timmers, C. M.; Turner, J. J.; Ward, C. M.; van der Marel, G. A.; Kouwizjer, M. L. C. E.; Grootenhuys, P. D. J.; van Boom, J. H. *Chem. Eur. J.* **1997**, *3*, 920. (b) Szabo, L.; Smith, B. L.; McReynolds, K. D.; Parrill, A. L.; Morris, E. R.; Gervay, J. J. *Org. Chem.* **1998**, *63*, 1074. (c) Smith, M. D.; Long, D. D.; Martin, A.; Marquess, D. G.; Claridge, T. D. W.; Fleet, G. W. J. *Chem. Commun.* **1998**, 2041. (d) Smith, M. D.; Claridge, T. D. W.; Tranter, G. E.; Sansom, M. S. P.; Fleet, G. W. J. *Chem. Commun.* **1998**, 2039. (e) Long, D. D.; Smith, M. D.; Martin, A.; Marquess, D. G.; Claridge, T. D. W.; Fleet, G. W. J. *Tetrahedron Lett.* **1998**, *39*, 9293. (f) Smith, M. D.; Long, D. D.; Martin, A.; Marquess, D. G.; Claridge, T. D. W.; Fleet, G. W. J. *Tetrahedron Lett.* **1999**, *40*, 2191. (g) Long, D. D.; Hungerford, N. L.; Smith, M. D.; Brittain, D. E. A.; Marquess, D. G.; Claridge, T. D. W.; Fleet, G. W. J. *Tetrahedron Lett.* **1999**, *40*, 2195. (h) Hungerford, N. L.; Claridge, T. D. W.; Aplin, R. T.; Moreno, A.; Fleet, G. W. J. *J. Chem. Soc., Perkin Trans. 1* **2000**, 3666. (i) Brittain, D. E. A.; Watterson, M. P.; Claridge, T. D. W.; Smith, M. D.; Fleet, G. W. J. *J. Chem. Soc., Perkin Trans. 1* **2000**, 3655. (j) Chakraborty, T. K.; Jayaprakash, S.; Srinivasu, P.; Govardhana Chary, M.; Diwan, P. V.; Nagaraj, R.; Ravi Sankar, A.; Kunwar, A. C. *Tetrahedron Lett.* **2000**, *41*, 8167. (k) Suhara, Y.; Yamaguchi, Y.; Collins, B.; Schnaar, R.; Yanagishita, M.; Hildreth, J. E. K.; Shimada, I.; Ichikawa, Y. *Bioorg. Med. Chem.* **2002**, *10*, 1999. (l) Gruner, S. A. W.; Truffault, V.; Voll, G.; Locardi, E.; Stöckle, M.; Kessler, H. *Chem. Eur. J.* **2002**, *8*, 4365.
- (8) (a) Graf von Roeder, E.; Lohof, E.; Hessler, G.; Hoffman, M.; Kessler, H. *J. Am. Chem. Soc.* **1996**, *118*, 10156. (b) Lohof, E.; Planker, E.; Mang, C.; Burkhardt, F.; Dechantreiter, M. A.; Haubner, R.; Wester, H. J.; Schwaiger, M.; Hölzemann, G.; Goodman, S. L.; Kessler, H. *Angew. Chem., Int. Ed.* **2000**, *39*, 2761. (c) Gruner, S. A. W.; Kéri, G.; Schwab, R.; Venetianer, A.; Kessler, H. *Org. Lett.* **2001**, *3*, 3723. (d) Chakraborty, T. K.; Jayaprakash, S.; Diwan, P. V.; Nagaraj, R.; Jampani, S. R. B.; Kunwar, A. C. *J. Am. Chem. Soc.* **1998**, *120*, 12962. (e) Chakraborty, T. K.; Ghosh, S.; Jayaprakash, S.; Sharma, J. A. R. P.; Ravikanth, V.; Diwan, P. V.; Nagaraj, R.; Kunwar, A. C. *J. Org. Chem.* **2000**, *65*, 6441. (f) Smith, A. B.; Sasho, S.; Barwis, B. A.; Sprengeler, P.; Barbosa, J.; Hirschmann, R.; Cooperman, B. S. *Bioorg. Med. Chem. Lett.* **1998**, *8*, 3133. (g) Overkleeft, H. S.; Verhelst, S. H. L.; Pieterman, E.; Meeuwenoord, N. J.; Overhand, M.; Cohen, L. H.; van der Marel, G. A.; van Boom, J. H. *Tetrahedron Lett.* **1999**, *40*, 4130. (h) Aguilera, B.; Siegal, G.; Overkleeft, H. S.; Meeuwenoord, N. J.; Rutjes, F. P. J. T.; van Hest, J. C. M.; Schoemaker, H. E.; van der Marel, G. A.; van Boom, J. H.; Overhand, M. *Eur. J. Org. Chem.* **2001**, 1541. (i) El Oualid, F.; Bruining, L.; Leroy, I. M.; Cohen, L. H.; van Boom, J. H.; van der Marel, G. A.; Overkleeft, H. S.; Overhand, M. *Helv. Chim. Acta* **2002**, *85*, 3455. (j) Chakraborty, T. K.; Jayaprakash, S.; Srinivasu, Madhavendra, S. S.; Ravi Sankar, A.; Kunwar, A. C. *Tetrahedron* **2002**, *58*, 2853.
- (9) McDevitt, J. P.; Lansbury, P. T., Jr. *J. Am. Chem. Soc.* **1996**, *118*, 3818.
- (10) (a) van Well, R. M.; Overkleeft, H. S.; Overhand, M.; Vang Carstensen, E.; van der Marel, G. A.; van Boom, J. H. *Tetrahedron Lett.* **2000**, *41*, 9331. (b) van Well, R. M.; Overkleeft, H. S.; Overhand, M.; van der Marel, G. A.; Bruss, D.; de Groot, P. G.; van Boom, J. H. *Bioorg. Med. Chem. Lett.* **2003**, *13*, 331.

- (11) (a) Haubner, R.; Finsinger, D.; Kessler, H. *Angew. Chem., Int. Ed. Engl.* **1997**, *36*, 1375. (b) Ojima, I.; Chakravarty, S.; Dong, Q. *Bioorg. Med. Chem.* **1995**, *3*, 337.
- (12) *NMR of proteins and nucleic acids*; Wüthrich, K., Ed.; Wiley: New York, 1986; Chapter 7, p 123.
- (13) *NMR of proteins and nucleic acids*; Wüthrich, K., Ed.; Wiley: New York, 1986; Chapter 2, p 17.
- (14) The variable temperature experiments were carried out in H₂O, and the observed $-\Delta\delta/\Delta T$ values of the NH of the SAA residues are comparable with those values found in other structured and unstructured linear SAA containing oligomers.^{8j}

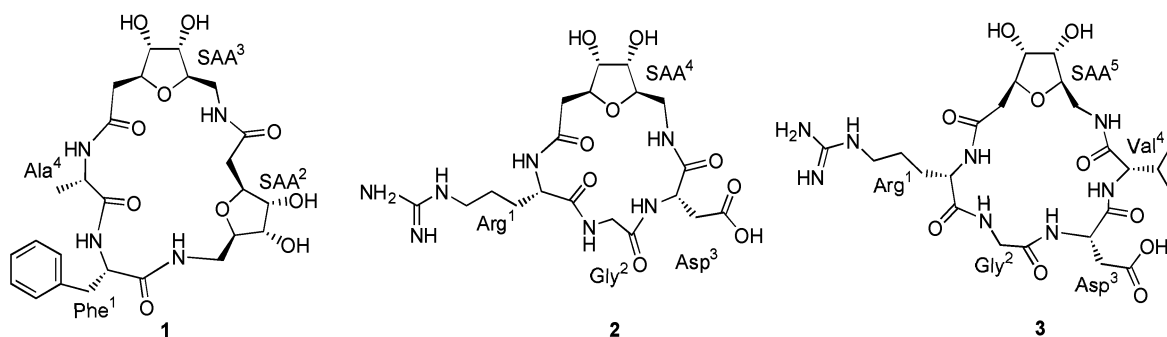


Figure 2. Furanoid ϵ -SAA III containing cyclic peptides 1–3.

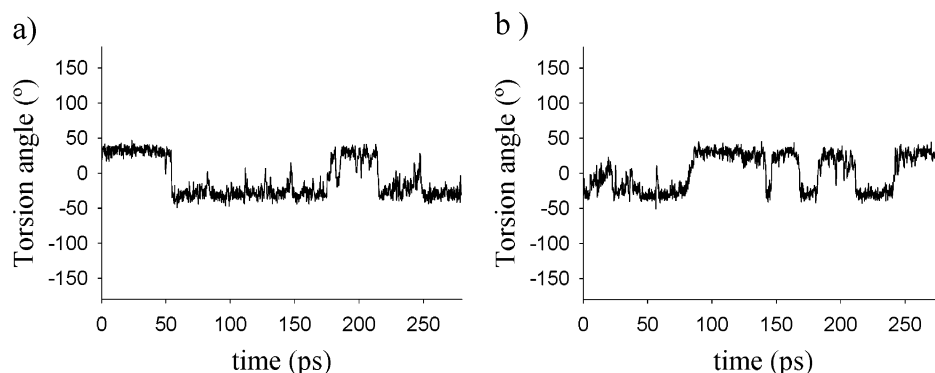


Figure 3. Behavior of the torsion angle C3–C4–C5–C6 of (a) SAA² and (b) SAA³ during MDtar. A positive torsion angle denotes a north conformer, and a negative torsion angle denotes a south conformer.

DG and MD Simulation. DG calculations with a modified^{15a} version of the program DISGEO^{15b,c} were used to generate a starting structure for the subsequent molecular dynamics simulations. The resulting ensemble of 100 structures showed a high degree of convergence, with the exception of the orientation of the amide proton of Phe¹. In roughly 60% of the conformers, Phe¹HN is solvent exposed. This conformation is supported by the presence of a strong ROE between Phe¹HN and its H β and by the presence of medium ROEs between Phe¹HN and the aromatic ring protons but conflicts with the strong ROE observed between Phe¹HN and SAA²HN. The apparently contradictory ROEs are indicative of the presence of at least two conformations in solution. Hence, it is incorrect to treat the ROEs as fixed distances, and we therefore decided to use an MD simulation using time-averaged distance restraints (tar) in which the experimental restraints need to be fulfilled over a period of time rather than instantaneously.¹⁶ The DG structure with the smallest total error was used as the starting geometry for the 280 ps MDtar calculation, which was carried out in explicit water using the CVFF force field¹⁷ of the Discover program. The resulting ensemble of structures fulfilled the ROE restraints, with no violations greater than 0.2 Å (see Table 4, Supporting Information). Analysis of the trajectory of the MDtar showed that SAA³ adopted an unusual nine-member β -turn-like arrangement stabilized by an intrasidue H bond between the amide proton and carbonyl oxygen of SAA³. The highest

conformational flexibility was exhibited by the Ala-Phe residues: during the simulation, the Ala⁴-Phe¹ amide bond flipped several times between a conformation with Phe¹HN oriented inward and Phe¹HN oriented outward. Depending on the conformation of the Ala-Phe region, the amide proton of SAA² was involved in an H bond interaction with the carbonyl oxygen of either alanine or SAA³. These hydrogen bonds were populated during the MDtar to a degree of 27% and 20%, respectively.¹⁸ The hydrogen-bonding interactions of the amide protons of both SAA residues were corroborated by the small temperature dependence of their chemical shifts.

Analysis of the furanoid ring of the two SAAs during the MDtar simulation revealed that they behaved differently (Figure 3). The five-member ring of SAA² started in an envelope conformation with C4 in the exo position (adopted nucleic acid nomenclature),¹⁹ but flipped to a twist conformation with C4 endo and C3 exo after only ± 50 ps. During the remaining 230 ps, it occupied mostly a twist or an envelope conformation with C4 endo. According to the concept of pseudorotation,²⁰ this conformation corresponds to a south conformation with a pseudorotational phase angle (P , defining the part of the ring which is most puckered) of 154° and a puckering amplitude (Φ_m , indicating the extent of puckering) of 35.6° . In contrast, the furanoid ring of SAA³ did not occupy a single stable conformation during the simulation but flipped between two different twist conformations (Figure 3b), i.e., 5_4T (a north conformation with C5 endo and C4 exo) and 4_3T (a south confor-

- (15) (a) Mierke, D. F.; Kessler, H. *Biopolymers* **1993**, 33, 1003. (b) Havel, T. F. *Prog. Biophys. Mol. Biol.* **1991**, 56, 43. (c) Havel, T. F. *Quantum Chemistry Program*, Exchange No. 507; Indiana University, 1988.
(16) Torda, A. E.; Scheek, R. M.; van Gunsteren, W. F. *J. Mol. Biol.* **1990**, 214, 223.
(17) (a) Maple, J. R.; Dinur, U.; Hagler, A. T. *Proc. Natl. Acad. Sci. U.S.A.* **1988**, 85, 5350. (b) Dauber-Osguthorpe, P.; Roberts, V. A.; Osguthorpe, D. J.; Wolff, J.; Genest, M.; Hagler, A. T. *Proteins: Struct., Funct., Genet.* **1988**, 4, 31.

- (18) The H bond population has been calculated accepting a distance between the donor and the acceptor of < 3.2 Å and an angle between the vectors CO and NH of $180 \pm 70^\circ$.
(19) *Structure and conformation of nucleic acids and protein–nucleic acid interactions*; Sundaralingam, M.; Rao, S. T., Eds.; University Park Press: Baltimore, 1974; Part 5, p 487.
(20) (a) Altona, C.; Sundaralingam, M. *J. Am. Chem. Soc.* **1972**, 94, 8205. (b) Altona, C.; Sundaralingam, M. *J. Am. Chem. Soc.* **1973**, 95, 2333

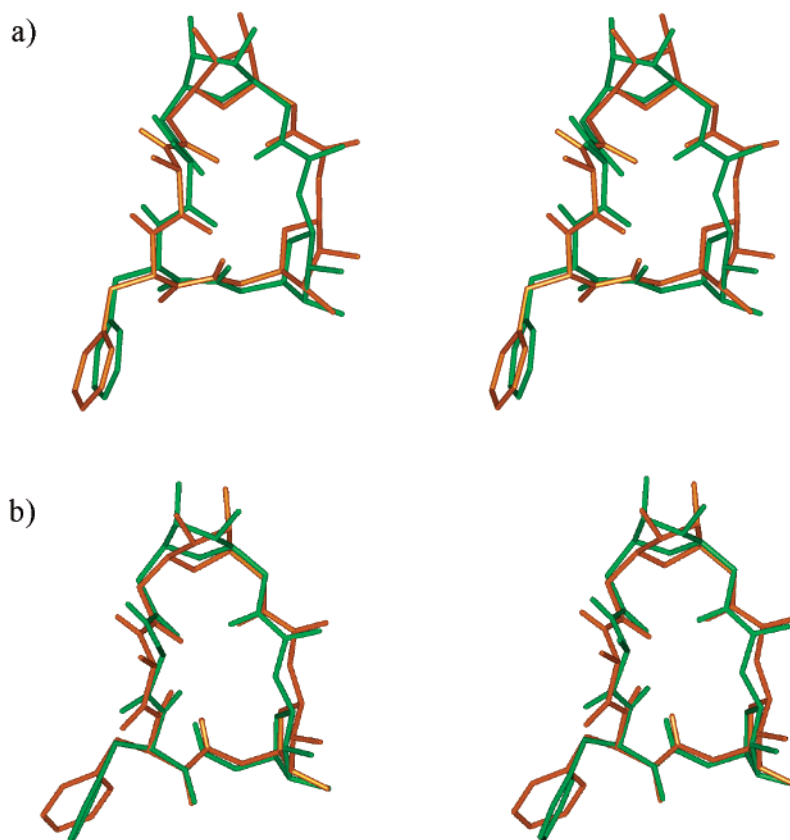


Figure 4. Stereopictures of a superposition of (a) two conformers of **1** having Phe¹HN oriented outward and SAA³ in a north (green) or a south (orange) conformation and (b) two conformers of **1** with Phe¹HN oriented inward and SAA³ in a north (green) or a south (orange) conformation. In all four conformers there is a hydrogen bond between HN and C=O of SAA³.

mation with C4 endo and C3 exo). Hence, four comparable conformations could be observed during the simulation, which varied in the orientation of the Ala-Phe amide bond and the ring conformation of SAA³ (Figure 4).²¹ In all four conformations, SAA³ adopted the H bond-stabilized nine-member turn structure. Analysis of the H bond population during the MDtar revealed a high stability of this turn structure as the intraresidue H bond was present to a degree of 73%.¹⁸

Empirical Calculations on the SAA Residues. The J coupling data were used to evaluate the furanoid ring conformations of the two ϵ -SAA residues resulting from the MDtar calculations. Given a complete set of coupling constants $J_{3,4}$, $J_{4,5}$, and $J_{5,6}$, the ring conformation can be calculated with the empirical PSEUROT program.²² The program is based on the concept that five-member rings are not frozen in a given conformation, but exist in an equilibrium between a north and a south conformation. On the basis of the three-bond coupling constants, P and Φ_m of the two conformers as well as their ratio can be determined. The required coupling constants were obtained by measuring 1D spectra in 10% D₂O in H₂O at 278, 283, and 298 K. The J couplings as measured in the spectra were refined using a simulation program from Perch software

to eliminate second-order effects.²³ The results from the PSEUROT calculations indicated that SAA² adopted almost exclusively a south conformation (95%) with a P of 130.1° and a Φ_m of 33.5°, located on the pseudorotational pathway between a ³E and ³₄T conformation. On the other hand, SAA³ had a N/S ratio of 40/60, with a P of ~0° (Φ_m = 36–40°) for the north conformation and a P of ~100° (Φ_m = 36–40°) for the south conformation. These results were in agreement with those from the MDtar simulation, although the calculated south conformation of SAA³ (i.e., ⁰₃T) differed slightly from the MDtar result (i.e., ⁴₃T).

The rotamer populations of the C2–C3 and C6–C7 bonds were calculated on the basis of the coupling constants using a generalized Karplus equation.²⁴ The calculations confirmed the conformations found in the MDtar simulation. Thus, in SAA² a –synclinal (–sc) conformation was found for C2–C3 as well as for C6–C7. On the other hand, C2–C3 adopted a +sc conformation in SAA³, whereas C6–C7 adopted a –sc conformation (see Figure 5).²⁵ The rotamer conformations in SAA³

(21) As diastereotopic assignment of the β protons in the Phe¹ side chain was impossible, information about its orientation was lost. Therefore, the conformation of the Phe side chain could not be calculated and the depicted structures are not representative concerning its orientation.

(22) (a) van Wijk, J.; Haasnoot, C. A. G.; de Leeuw, F. A. A. M.; Huckriede, B. D.; Westra Hoekzema, A.; Altona, C. *PSEUROT 6.3*; Leiden Institute of Chemistry, Leiden University: The Netherlands, 1999. (b) de Leeuw, F. A. A. M.; Altona, C. *J. Comput. Chem.* **1983**, *4*, 428. (c) Altona, C. *Recl. Trav. Chim. Pays-Bas* **1982**, *101*, 413.

(23) (a) Laatikainen, R.; Niemitz, M.; Weber, U.; Sundelin, J.; Hassinen, T.; Vepsäläinen, J. *J. Magn. Reson.* **1996**, *A120*, 1. (b) Laatikainen, R.; Niemitz, M.; Malaisse, W. J.; Biesemans, M.; Willem, R. *Magn. Reson. Med.* **1996**, *36*, 359.

(24) (a) Altona, C. *Vicinal Coupling Constants & Conformation of Biomolecules in Encyclopedia of NMR*; Grant, D. M., Harris, R. K., Eds.; Wiley: New York, 1996; p 4909. (b) van Wijk, J.; Huckriede, B. D.; Ippel, J. H.; Altona, C. *Furanose sugar conformations in DNA from NMR coupling constants*. In *Methods in Enzymology*; Lilley, D. J. M., Dahlberg, J. E., Eds.; Academic Press: San Diego, 1992; Vol. 211, p 286. (c) Altona, C.; Ippel, J. H.; Westra Hoekzema, A. J. A.; Erkelens, C.; Groesbeek, M.; Donders, L. A. *Magn. Reson. Chem.* **1989**, *27*, 564. (d) Altona, C.; Francke, R.; de Haan, R.; Ippel, J. H.; Daalmans, G. J.; van Wijk, J. *Magn. Reson. Chem.* **1994**, *32*, 670.

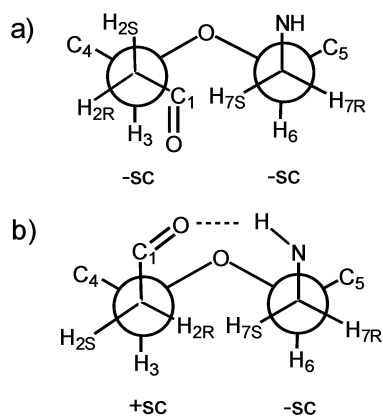


Figure 5. (a) Rotamer conformation around C2–C3 and C6–C7 in SAA². (b) Rotamer conformations in SAA³.

allow for the presence of an intrasidue hydrogen bond stabilizing nine-member turn structure. Such a hydrogen-bonding interaction is not possible with the rotamer conformations found for the methylene functions of SAA² (Figure 5).

Crystal Structure of Compound 1. The asymmetric unit contains two independent copies of the cyclic tetramer together with seven ordered water molecules. Superposition of the two copies indicated them to be virtually identical (RMSD = 0.2 Å). Figure 6a shows a stereopicture of one of the copies. The crystal structure strongly resembles the solution-phase conformers. SAA³ forms the simulated turn structure, stabilized by a nine-member intrasidue hydrogen bond between the amide proton and the carbonyl oxygen. The furanoid ring of SAA³ adopts a north conformation with C5 in the endo position, contrary to the slight preference for a south conformation in solution as established in the NMR-based calculations. SAA² adopts the same conformation in the crystal structure as found in all four solution conformers (Table 2). The largest deviation between the crystal and solution conformations can be found in the Phe-SAA² amide bond, as shown in Figure 6b. In the crystal structure, the amide proton of SAA² is involved in a hydrogen bond with the carbonyl oxygen of SAA³, whereas this hydrogen bond is populated in solution only to about 20%. A superposition of the X-ray structure with the solution conformation with Phe¹HN oriented outward considering the backbone atoms gives an RMSD of 0.44 (Figure 6b). It is convincing to see such an agreement between X-ray and NMR; however, we have to keep in mind that principally there might be dramatic differences between structures in crystal and solution.²⁶

Conformational Analysis of cyclo[Arg-Gly-Asp-SAA] 2. **NMR Analysis.** The ¹H NMR spectra of compound 2, recorded as described for compound 1, showed the presence of one set of resonance signals that were assigned using a combination of COSY, TOCSY, and ROESY experiments. Diastereotopic assignment of the prochiral methylene protons at C2 of the SAA residue was done on the basis of the *J*_{2,3} coupling constants and ROEs. Because of signal overlap, the coupling constants for the methylene protons at C7 could not be determined. The stereospecific assignment of H_{7R} and H_{7S} was accomplished by testing both prochiral assignments for ROE restraint violations during the DG calculations.²⁷ The ROESY spectrum (τ_{mix}

= 180 ms) displayed 32 distinct ROE cross-peaks, which were converted into interproton distances for the calculations. The four strong sequential H α /HN cross-peaks imply an all-trans conformation of the peptide bonds. Two HN/HN peaks were observed, attributable to interactions between Gly²HN/Asp³HN and Asp³HN/SAA⁴HN. The ³*J*_{HN,H α} coupling constants all lie within the uninformative region of the Karplus plot and as a consequence were not used in the ensuing calculations. The small magnitude (i.e., −1.6 ppb/K) of the SAA⁴HN temperature coefficient in compound 2, determined in H₂O, suggests that the amide proton is involved in intramolecular hydrogen bonding. The chemical shifts of the other three amide protons all displayed temperature shifts larger than −5 ppb/K.

DG and MD Simulation. The ensemble of 100 structures resulting from a DG calculation showed a high degree of convergence and fulfilled the distance restraints. The averaged and minimized structure of a 150 ps restrained MD (rMD) simulation at 300 K is depicted in Figure 7.²⁸ No violations larger than 0.15 Å occurred for any of the distance restraints. To test the stability and quality of the structure, a 150 ps free MD calculation in explicit water was performed. Superposition of the heavy atoms of the average structures from both the free and restrained simulations indicated that only small conformational changes occurred (RMSD = 0.36 Å). Analysis of the rMD trajectory showed the nine-member hydrogen bond-stabilized turn structure for SAA⁴ as found in compound 1. During the simulation, the furan ring of SAA⁴ adopted a south conformation (*P* ≈ 112) with C3 in the exo position. Because of partial overlap of the ring proton signals in the NMR spectra, the coupling constants could not be used to confirm these results. The +sc conformation around C2–C3, with both H_{2R} and H_{2S} gauche to H₃, is consistent with the experimental coupling constants (³*J*_{2S,3} = 5.1 Hz and ³*J*_{2R,3} = 3.2 Hz). The preferred rotamer for C6–C7 also has both methylene protons (H_{7R} and H_{7S}) in a gauche position relative to C6 (because of overlapping signals, the coupling constants could not be determined for H_{7R} and H_{7S}). These rotamer conformations place the amide proton and carbonyl oxygen of the SAA residue in the required orientation for the formation of an intrasidue hydrogen bond. The RGD sequence has a well-defined kinked conformation, with glycine in the center of the kink. However, the Φ and Ψ angles do not match the γ -turn observed in the α / β -selective cyclic RGD peptides (Table 3).²⁹ Particularly, in respect to such ligands, a 180° rotation of the Gly-Asp amide bond occurs in our compound, preventing the Asp-NH proton to be involved in a hydrogen bond to the receptor and leading to a nonoptimal orientation of the pharmacophoric aspartic acid side chain.

Conformational Analysis of cyclo[Arg-Gly-Asp-Val-SAA] 3. **NMR Analysis.** The 1D NMR spectrum of cyclo[Arg-Gly-Asp-Val-SAA] 3 displayed one set of resonances with well-resolved chemical shifts. A complete assignment of the proton resonances was obtained using ¹H NMR in combination with COSY, TOCSY, and NOESY experiments. Diastereotopic assignment of the methylene protons of the SAA residue was

(25) Klyne, W.; Prelog, V. *Experientia* **1960**, *16*, 521.

(26) Kessler, H.; Zimmerman, G.; Förster, H.; Engel, J.; Oepem, G.; Sheldrick, W. S. *Angew. Chem., Int. Ed. Engl.* **1981**, *20*, 1053.

(27) (a) Hanson, K. R. *J. Am. Chem. Soc.* **1966**, *88*, 2731. (b) Hirschmann, H.; Hanson, K. R. *J. Org. Chem.* **1971**, *36*, 3293.

(28) As diastereotopic assignment of the β protons in the side chains of Asp and Arg was impossible, information about the side chain orientation was lost. Therefore, the conformation of the Arg and Asp side chains could not be calculated and the depicted structures are not representative concerning their orientation.

(29) Dechantreiter, M. A.; Planker, E.; Mathä, B.; Lohof, E.; Hölzeman, G.; Jonczyk, A.; Goodman, S. L.; Kessler, H. *J. Med. Chem.* **1999**, *42*, 3033.

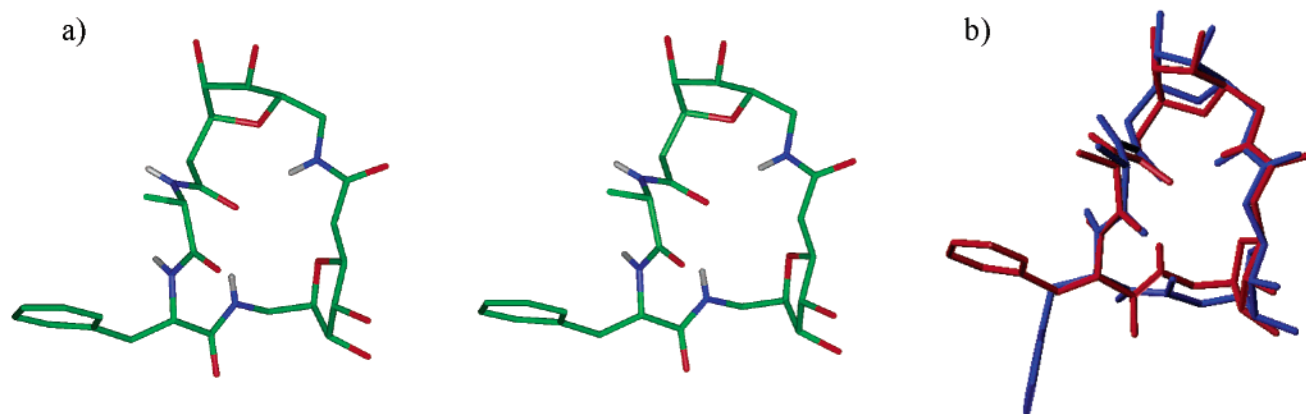


Figure 6. (a) Stereopicture of one of the copies in the asymmetric unit as determined by X-ray crystallography. (b) Superposition of the X-ray structure (red) with the solution conformation with Phe HN oriented outward (blue). In the superposition procedure, all the backbone atoms were considered. The RMSD is 0.44.

Table 2. Torsion Angles of the Five-Member Rings of the SAA Residues in **1** Resulting from the MD Calculations, PSEUROT Calculations, and X-ray Diffraction

torsion angle	SAA ²			SAA ³ north			SAA ³ south	
	MD	PSEUROT	X-ray	MD	PSEUROT	X-ray	MD	PSEUROT
C6–O–C3–C4	–25°	–31°	–30°	3°	20°	–8°	–28°	–37°
O–C3–C4–C5	36°	32°	39°	–24°	–35°	–14°	34°	26°
C3–C4–C5–C6	–32°	–22°	–34°	34°	36°	30°	–26°	–5°
C4–C5–C6–O	18°	2°	17°	–33°	–24°	–34°	10°	–18°
C5–C6–O–C3	5°	17°	8°	19°	3°	27°	11°	34°

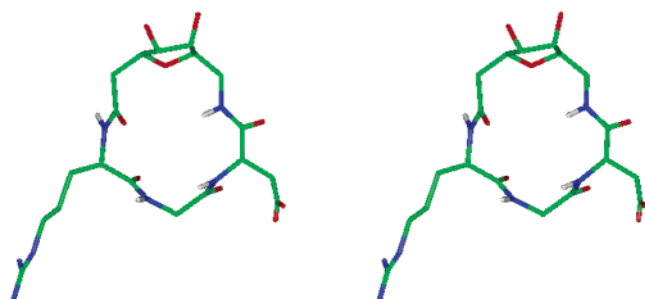


Figure 7. Stereopicture of a minimized (300 steps steepest descent) average conformation of **2** resulting from a 150 ps rMD calculation.

Table 3. Φ and Ψ Angles of RGD Sequence in **2**

	cyclo[RGD-SAA] 2	
	Φ	Ψ
Arg	–93	120
Gly	73	57
Asp	64	61

accomplished on the basis of 3J coupling constants and NOEs and by testing both prochiral assignments for violations of the NMR data during DG calculations. A total of 29 informative cross-peaks observed in the NOESY spectrum ($\tau_{\text{mix}} = 500$ ms) were used for the calculations. The absence of $\text{H}\alpha/\text{H}\alpha$ cross-peaks, together with the presence of strong sequential $\text{HN}/\text{H}\alpha$, indicated that all the backbone amide bonds adopted a trans conformation as expected. The NOESY spectrum displayed two interesting HN/HN cross-peaks representing $\text{Asp}^3\text{HN}/\text{Val}^4\text{HN}$ and $\text{Val}^4\text{HN}/\text{SAA}^5\text{HN}$ connectivities. Temperature dependence studies indicated that none of the amide protons are involved in intramolecular hydrogen bonding.

DG and MD Simulation. The ensemble of DG structures showed the presence of multiple conformers in solution. An

MDtar calculation confirmed that compound **3** is flexible with the largest structural variations in the orientation of the Gly–Asp amide bond, the rotamer conformation around C2–C3, and the ring pucker. The observed NMR data of **3** reflected the presence of several conformers (in fast exchange) in solution.

From the DG and MD calculations it became clear that SAA⁵ does not form the intrasidue H bond-stabilized turn structure as observed in compounds **1** and **2**. The conformational flexibility of compound **3** presumably arises from the presence of an additional amino acid residue (valine) as compared to compound **2**.

Discussion and Conclusion

The data obtained from conformational studies of compound **1** with MD simulations, X-ray crystallography, and empirical calculations generally agree well. The two sequential SAA residues in **1** adopt different conformations. SAA³ interchanges between a north (^5_4T) and a south ($^4_3\text{T}^0_3\text{T}$) conformation and forms an unusual turn structure stabilized by an internal nine-member hydrogen bond, regardless of the ring conformation. SAA² adopts an extended conformation with a different rotamer population around the C2–C3 bond (see Figure 5).³⁰

The cyclic-RGD peptide **2**, containing one furanoid ϵ -SAA residue III also adopts a preferred conformation in which the SAA residue forms the nine-member H-bonded turn structure. This unusual turn induces a kinked conformation in the RGD sequence which deviates from the standard β/γ -turn conformation usually observed in the corresponding cyclic pentapeptides³¹

(30) The possibility to fix the rotamer populations around the exocyclic methylene functions to predetermine the conformation of the ϵ -SAA residue is currently under investigation.

(31) (a) Kessler, H. *Angew. Chem., Int. Ed. Engl.* **1982**, *21*, 512. (b) Gurrath, M.; Müller, G.; Kessler, H.; Aumailley, M.; Timpl, R. *Eur. J. Biochem.* **1992**, *210*, 911.

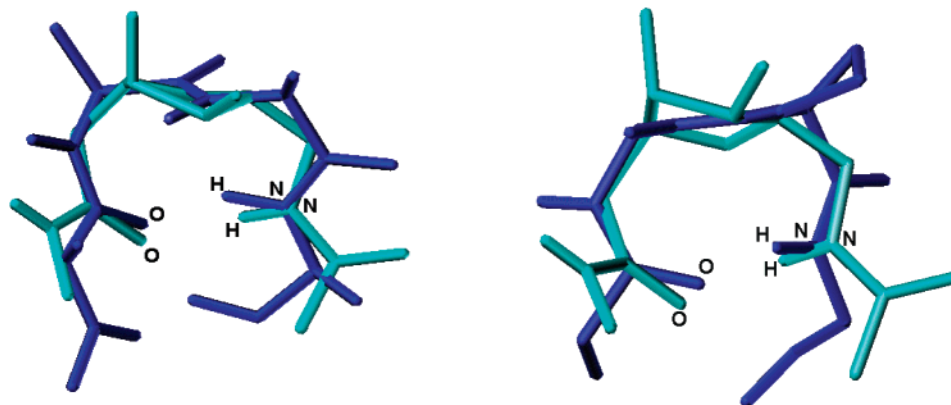


Figure 8. Superposition of the turn in **1** (cyan) as found by X-ray crystallography and the type I (blue) and VIa (blue) β -turns on the left and right, respectively.

and derivatives.³² RGD peptide **2** has a $\alpha_{\text{IIb}}\beta_3$ -selective ArgC β -AspC β distance (i.e., >7.5 Å),³³ which is in agreement with the previously established biological activity [$\text{IC}_{50}(\alpha_{\text{IIb}}\beta_3) = 384$ nM, $\text{IC}_{50}(\alpha_{\text{v}}\beta_3)/\text{IC}_{50}(\alpha_{\text{IIb}}\beta_3) = 3.9$].^{10b}

Compound **3** contains an additional valine residue as compared to **2**, and this extension apparently excludes the formation of a preferred conformation. The more flexible character of **3**, compared to **2**, may cause the decrease in affinity for the integrin receptors [$\text{IC}_{50}(\alpha_{\text{IIb}}\beta_3) = 32$ μM , $\text{IC}_{50}(\alpha_{\text{v}}\beta_3)/\text{IC}_{50}(\alpha_{\text{IIb}}\beta_3) = 3.0$].^{10b}

Superposition of the SAA atoms C1, C2, C3, C6, C7, C8, and N in **1** (SAA³) and **2** (SAA⁴) reveals as high similarity of the two turns with an RMSD of only 0.33 Å. To determine if these turns are conformationally similar to any of the classical turn types, the X-ray structure was compared with idealized β -turns (types I, I', II, II', III, III', VIa, VIb) at eight atom positions (O, C1, C2, C3, C6, C7, N, NH of **1** and the corresponding O_i, C_i, N_{i+1}, C_{i+1}, C_{i+2}, N_{i+3}, HN_{i+3} of ideal turns). The RMSD values from such a comparison are as follows: 0.57 for type I, 0.65 for type I', 0.62 for type II, 0.60 for type II', 0.53 for type III, 0.67 for type III', 0.40 for type VIa, and 0.64 for type VIb. It appears that SAA **III** conformationally resembles the type VIa β -turn, but types I and III show a good fit as well (Figure 8). However, with respect to the classical β -turns, which contain a ten-member ring H bond, SAA **III** forms an internal nine-member ring H bond. In addition, the direction of the peptide backbone in the ϵ -SAA **III** turn is reversed (Figure 9). In this respect, ϵ -SAA **III** differs from δ -SAAs^{7a,b,h} of type **I** that are known to form β -turns with the SAA residue in the $i + 1$ and $i + 2$ positions of the turn.³⁴

In summary, SAA **III** forms a novel unusual intraresidue nine-member H-bonded turn structure, resembling the retro version of a type VIa β -turn. The results reported here provide detailed structural information necessary for the design of SAA-containing molecules with predetermined structures in the

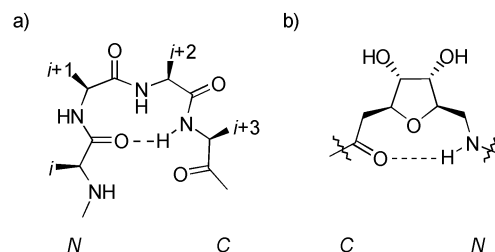


Figure 9. Comparison between (a) a ten-member ring structure of a β -turn and (b) the nine-member ring structure of the ϵ -furanoid SAA.

development of biologically active molecules and foldamers³⁵ with interesting properties.

Experimental Section

NMR Measurements. All spectra were recorded at 278K on a Bruker DMX 600 or a Bruker DMX 500 spectrometer equipped with a pulsed field gradient accessory in H₂O/D₂O (9/1, v/v). Standard DQF-COSY (512c \times 2084c) and TOCSY (400c \times 2048c) spectra were recorded using presaturation for solvent suppression. ROESY spectra (400c \times 2048c, $\tau_{\text{mix}} = 180$ ms) were recorded using the watergate solvent suppression.³⁶ All spectra were recorded in phase-sensitive mode, using either the TPPI or states-TPPI for quadrature detection in the indirect dimension. Interproton distances were obtained from ROESY or NOESY experiments. Integration of the cross-peaks was performed with X-winnmr, and the resulting integrals were offset corrected³⁷ (in the case of ROESY experiments). The isolated spin-pair approximation was used, setting the integrated intensity of the NOE cross-peak derived from a set of geminal protons of the SAAs to a distance of 1.78 Å. The upper and lower bond restraints were set as distance $\pm 10\%$, accounting for the experimental error. Regions on both sides of the diagonal were analyzed, and when the cross-peak volumes did not coincide, the smallest lower bound and highest upper bound of the two sets of distance restraints were used. Pseudoatom corrections were taken into account. Homonuclear coupling constants were determined from the corresponding ¹H spectra. The coupling constants of the furan ring protons were determined at 278, 283, and 298 K and refined using a Perch software simulation program. The temperature dependence of the chemical shifts of the amide protons was measured by recording 1D spectra in the range 275–320 K as an indication of solvent accessibility.

(32) A cyclic-modified peptide, containing a structurally related ϵ -amino acid having a thiophene ring rather than a furanoid ring and three amino acids, adopts a totally different conformation: Feigel, M.; Lugert, G.; Heichert, C. *Liebigs Ann. Chem.* **1987**, 367.

(33) (a) Pfaff, M.; Tangemann, K.; Müller, B.; Gurrath, M.; Müller, G.; Kessler, H.; Timpl, R.; Engel, J. *J. Biol. Chem.* **1994**, 269, 20233. (b) Müller, G.; Gurrath, M.; Kessler, H. *J. Comput.-Aided Mol. Des.* **1994**, 8, 709.

(34) A pyranoid ϵ -SAA incorporated as a scaffold in a mammalian ribonucleotide reductase inhibitor was shown to be able to adopt a conformation similar to the β -turn conformation of the parent heptapeptide with the SAA replacing the $i + 1$ and $i + 2$ residues of the turn.^{8f} It is not excluded that a nine-member intraresidue H bond interaction can also be observed in this ϵ -SAA-containing peptide.

(35) (a) Gellman, S. H. *Acc. Chem. Res.* **1998**, 31, 173. (b) Seebach, D.; Matthews, J. L. *Chem. Commun.* **1997**, 2015. (c) Gademann, K.; Hintermann, T.; Schreiber, J. V. *Curr. Med. Chem.* **1999**, 6, 905. (d) DeGrado, W. F.; Schneider, J. P.; Hamuro, Y. *J. Pept. Res.* **1999**, 54, 206. (e) Hill, D. J.; Mio, M. J.; Prince, R. B.; Hughes, T. S.; Moore, J. S. *Chem. Rev.* **2001**, 101, 3893.

(36) Piotto, M.; Saudek, V.; Sklenar, V. *J. Biom. NMR* **1992**, 2, 661.

(37) Bax, A. *J. Magn. Reson.* **1988**, 77, 134.

Computer Simulations. All molecular modeling calculations were performed on a Silicon Graphics O2 using the program InsightII. A DG calculation was performed to generate a starting conformation for MD calculations. A modified^{15a} version of the program DISGEO,^{15b,c} in combination with interproton distances and $J_{\alpha,\beta}$ of the natural amino acids, was employed for the DG. The resulting structure was placed in a cubic box with a box length of 40 Å, which was soaked with H₂O molecules. The MD calculations were performed with the aid of the Discover program using the CVFF force field.¹⁷ A dynamics simulation of 280 ps duration, using a self-written extension for time-averaged distance restraints, was performed for compound **1**. The force constant on distance restraints was set to 10 kJ·mol⁻¹, and a decay constant τ of 28 ps was used. The calculation was done with the explicit-image model of periodic boundary conditions. During the trajectory, four different conformations could be observed, and each structure was minimized with 300 steps of the steepest-descent algorithm, yielding the structures depicted in Figure 4. The pseudorotation parameters of the two stable conformers of the furan rings in **1** and the mole fractions were calculated with the iterative least-squares program PSEUROT 6.3.²² The Diez–Donders-extended Karplus equation, in combination with $^3J(\text{H}^3\text{H}^4)$, $^3J(\text{H}^4\text{H}^5)$, and $^3J(\text{H}^6\text{H}^7)$ determined at three different temperatures, were used for the calculations, which were performed on a PC. For the RGD compound **2**, the MD calculations consisted of two parts, a restrained MD part and a free MD without restraints. After energy minimization using steepest descent and a conjugate gradient, the system was gradually heated starting from 10 K and increasing to 50, 100, 150, 200, 250, and 300 K in 1 ps steps. The system was equilibrated for 25 ps with temperature-bath coupling. Configurations were saved every 100 fs for 150 ps during the dynamics to obtain the trajectory, which was averaged and minimized with a 300 steps steepest-descent algorithm to afford the structure depicted

in Figure 7. A time-averaged MD simulation as described for compound **1** was also performed for compound **3**. The simulation was run for 300 ps with a τ of 30 ps. The distance restraints and their violations for the three MD calculations are listed in Tables 1, 2, and 3 in the Supporting Information.

Crystallization and Structure Solution of cyclo[Phe-SAA-SAA-Ala] **1.** Colorless needle-shaped crystals of compound **1** were obtained after three months of slow evaporation of 5 μL droplets of 30 mg/mL peptide in water under paraffin oil in Terazaki plates. Faster evaporation under air or vapor diffusion using common protein precipitants was not successful. The crystal used for data collection was $0.08 \times 0.12 \times 1.2$ mm and was mounted in air. Wider crystals could not be grown. Data were collected to 0.8 Å resolution, and the structure was solved using the SnB program.³⁸ Refinement was done using SHELX97.³⁹ The relatively poor refinement statistics are presumably due to the crystals shape, leading to poor absorption correction.

Acknowledgment. The authors thank Gijs van der Marel and Hermen Overkleeft for helpful discussions. Gregg Siegal acknowledges the Dutch Royal Academy of Sciences for fellowship support.

Supporting Information Available: ¹H spectral data for compounds **1**, **2**, and **3** and comparisons between the experimentally determined and simulated NOE-derived distances for **1**, **2**, and **3** (PDF and CIF). This material is available free of charge via the Internet at <http://pubs.acs.org>.

JA035461+

(38) Weeks, C. M.; Miller, R. J. *Appl. Crystallogr.* **1999**, 32, 120.

(39) Herbst-Irmer, R.; Sheldrick, G. M. *Acta Crystallogr., Sect. B* **1998**, 54, 443.